

Efficient Reduction of Chitosan Molecular Weight by High-Intensity Ultrasound: Underlying Mechanism and Effect of Process Parameters

TAO WU,[†] SVETLANA ZIVANOVIC,^{*,†} DOUGLAS G. HAYES,[‡] AND JOCHEN WEISS[§]

Food Biopolymers Research Group, Department of Food Science and Technology, The University of Tennessee, 2509 River Drive, Knoxville, Tennessee 37996-4539; Department of Biosystems Engineering and Soil Science, The University of Tennessee, 2506 E. J. Chapman Drive, Knoxville, Tennessee 37996-4531; and Food Biophysics and Nanotechnology Laboratory, Department of Food Science, Chenoweth Laboratory 234, University of Massachusetts, Amherst, Massachusetts 01003

The degradation of chitosan by high-intensity ultrasound (HIU) as affected by ultrasound parameters and solution properties was investigated by gel permeation chromatography coupled with static light scattering. The molecular weight, radius of gyration, and polydispersity of chitosan were reduced by ultrasound treatment, whereas chitosan remained in the same random coil conformation and the degree of acetylation did not change after sonication. The results demonstrate that (1) the degradation of chitosan by ultrasound is primarily driven by mechanical forces and the degradation mechanism can be described by a random scission model; (2) the degradation rate is proportional to M_w^0 ; and (3) the degradation rate coefficient is affected by ultrasound intensity, solution temperature, polymer concentration, and ionic strength, whereas acid concentration has little effect. Additionally, the data indicate that the degradation rate coefficient is affected by the degree of acetylation of chitosan and independent of the initial molecular weight.

KEYWORDS: Chitosan; molecular weight; degradation; high-intensity ultrasound; random scission model

INTRODUCTION

Commercial application of chitosan is closely associated with its functional properties and biological activities, which are primarily governed by two structural properties: the molecular weight (MW) and degree of acetylation (DA). However, the MW of commercially available chitosan is greatly affected by the source and the extraction and production methods. It varies widely between manufacturers and even between batches of the same manufacturer. With the aim of producing chitosan of desired MW, various methods, including acid and enzyme hydrolysis, microwave, UV, and γ irradiation, as well as high-intensity ultrasound (HIU), have been investigated (1–4).

HIU has received much attention as a rapid, environmentally friendly, and byproduct-free method. The mechanism, kinetics, and application of ultrasound in the degradation of various synthetic polymers have been widely investigated (5–8). Cleavage of polymer chains by HIU with frequencies ranging from 20 to 100 kHz has been attributed mainly to the action of shear forces formed due to the relative movement between solvent

and polymer molecules during the collapse of cavitation bubbles and the formation of microjets (5). Thus, the underlying cause of degradation of a polymer by ultrasound is considered to be primarily of a mechanical nature. However, at frequencies higher than 100 kHz, free HO* radicals formed by ultrasound in an aqueous solution have a significant role in the polymer degradation (9). Czechowska et al. used 360 kHz ultrasound treatment to degrade chitosan and found that the chain scissions were induced by both mechanical forces and free radicals (10). At the same time, side reactions leading to the formation of carbonyl groups were observed (10).

Two types of factors, ultrasound parameters (including frequency and intensity) and solution properties (solvent, temperature, nature of dissolved gas, nature of polymer, etc.) have been found to affect the degradation process of polymers (5, 8). Due to the polydisperse nature of most polymers, an accurate analysis of the degradation kinetics is almost impossible without information about the location of chain scission and the dependence of rate coefficients on the molecular weight of the polymer (5). Two simplified models, based on different assumptions of the location of chain scission, have been proposed to quantitatively describe the degradation process of polymers.

(I) Random Scission Polymer Degradation Model. One of the earliest models was developed by Schmid; the author assumed that the scission of polymer chains occurs randomly and that the rate of degradation decreases with decreasing chain

* Corresponding author [telephone (865) 974-0844; e-mail: svetlanaz@utk.edu].

[†] Department of Food Science and Technology, The University of Tennessee.

[‡] Department of Biosystems Engineering and Soil Science, The University of Tennessee.

[§] University of Massachusetts.

length (l). By the same assumption, the rate of degradation reaches zero at M_c , the final limiting molecular weight, below which no further degradation can occur. Thus

$$\frac{M_c}{M_t} + \ln\left(1 - \frac{M_c}{M_t}\right) = -\frac{k_1}{c}\left(\frac{M_c}{m}\right)^2 \times t + \frac{M_c}{M_i} + \ln\left(1 - \frac{M_c}{M_i}\right) \quad (1)$$

where M_i , M_c , and M_t represent the initial and final number-average molecular weights and the number-average molecular weight after sonication time (t), respectively; m refers to the molecular weight of the monomer, c to the initial molar concentration of the polymer, and k_1 to the degradation rate coefficient.

(II) Midpoint Chain Scission Polymer Degradation Model.

Assuming the degradation occurs at the midpoint of the polymer chain, a continuous distribution model has recently been developed (12). For a polymer with chain length x , the overall degradation with a rate constant k_2 can be described as

$$P(x) \xrightarrow{k_2} 2P\left(\frac{x}{2}\right) \quad (2)$$

The evolution of the number-average molecular weight with sonication time is thus given by

$$\ln\left[\frac{M_i - M_c}{M_t - M_c}\right] = k_3 M_c t \quad (3)$$

where k_3 refers to the degradation rate coefficient. Baxter et al. suggested that the chain scission of chitosan by ultrasound occurs randomly and follows the Schmid model (13), whereas Trzcinski and Staszewska argued that a bimodal molecular distribution is obtained at early stages of degradation, suggesting that the chain scission is not random but occurs at the midpoint of the chain (14). However, in both studies kinetics of ultrasonic degradation has been determined by using the viscosity-average molecular weight, although both models (eqs 1 and 3) require that molecular weights are expressed as number-average.

High-intensity ultrasound has been widely investigated for the degradation of chitosan. In general, it has been found that HIU reduces the molecular weight, radius of gyration, and polydispersity of chitosan efficiently without affecting its DA values (1, 13, 15). Interestingly, it has also been reported that with intensive sonication, the degree of acetylation of chitosan increases (i.e., chitosan is actually being acetylated) if the initial DA is $>10\%$ and stays unchanged if it is $<10\%$ (16). Similarly to the degradation behavior of synthetic polymers, chitosan degrades more rapidly in dilute solutions and at low temperatures (1, 14, 15), whereas the type of solvent has no significant influence on the degradation rate (1). However, Trzcinski et al. found that the increase of acetic acid concentration from 0.1 to 1 M results in a higher rate coefficient (14), whereas Li et al. stated that optimal degradation conditions occur at the lowest acetic acid concentration (15). The initial molecular weight and degree of deacetylation have been found to affect the degradation process—chitosan samples with high molecular weight and low DA are easily degradable by HIU (16, 17).

In summary, despite significant efforts in this area, contradictory results can be found in the literature. In most studies, the actual ultrasound intensity has not been determined and, consequently, these results are not only hard to compare but are of little use for industry to scale up the process. Additionally, most of the published studies have monitored the degradation process by determination of the viscosity-average molecular

weight, which lacks information of absolute molecular weight and cannot be used to analyze kinetics mechanisms. This is possibly the main reason for the conflicting results in the literature. A comprehensive study was conducted here with the objective to determine the effects of HIU parameters (intensity and treatment time) and solution properties (temperature, chitosan concentration, acetic acid concentration, ionic strength, and chitosan initial DA and molecular weight) on the ultrasound degradation of chitosan using gel permeation chromatography (GPC) derived values of molecular weight. Additionally, a simplified approach to predict the change of molecular weight has been derived, which can be used as a guideline for the industrial application of HIU in the degradation of chitosan.

EXPERIMENTAL DETAILS

Materials. Chitosan samples with various degrees of acetylation (19, 29, and 39% DA as labeled by the manufacturer) were kindly donated by Primex (Primex Co., Iceland). Water-soluble chitosan was purchased from EZ Life Science Co. Ltd. (Seoul, South Korea). Other chemicals were purchased from Fisher Scientific (Pittsburgh, PA). All chitosan samples were analyzed for weight-average molecular weight (M_w) and DA according to methods described below.

Chitosan Solution Preparation. Chitosan solutions, 0.25, 0.5, 1, and 2% (w/v), were freshly prepared in 1% (v/v) aqueous acetic acid. Ionic strength of 1% chitosan solution was adjusted to 0.1 and 0.2 M by adding suitable amounts of sodium chloride. All chitosan solutions were filtered through Miracloth (rayon-polyester; EMD Bioscience, San Diego, CA) and kept in a refrigerator prior to sonication. Chitosan with 20.2% DA was used to investigate the effects of acoustic intensity and time, and 32.5% DA chitosan was used to investigate the effects of solution properties.

Ultrasound Treatment Procedure. One hundred milliliters of each chitosan solution was sonicated by a 20 kHz ultrasound generator (Sonics and Materials VC-750, Newton, CT) with a 0.5 in. titanium probe in pulse mode (30 s on, 30 s off) in 100 mL glass beakers. For evaluation of effects of sonication time and amplitude, the temperature control of the generator was set at 30 °C and the sample was kept in an ice–water bath during the experiment. For evaluation of effects of temperature, the temperature control was set at 30, 50, and 80 °C and the beakers with samples were placed in an iced water bath, an ambient temperature water bath, and ambient air, respectively. The sample temperature was monitored by a temperature probe during the entire ultrasound process. The temperature of solution increased when the sonication was on and dropped a few degrees when the sonication was off, but the maximum temperature did not exceed 30, 50, and 80 °C, corresponding to the preset values of the generator. The sonication time ranged from 5 to 60 min. A 1.0 mL aliquot of sonicated sample solution was taken at specified time intervals, diluted with the solvent, and analyzed by gel permeation chromatography (GPC). All of the presented data points were averages of at least two independent sonication experiments.

The ultrasonic intensity can be measured calorimetrically by measuring the time-dependent increase in temperature of sample in the ultrasonic reactor (18). However, the intensity of ultrasound can be simply controlled by setting the displacement (P_A) of the ultrasound generator probe. As P_A increases, both the number and size of cavities increase, resulting in an increased overall chemical and mechanical activity. On the basis of the manufacturer's manual, for a 13 mm threaded probe with a replaceable tip, the P_A set at 100% results in an amplitude of 124 μm and maximum power output. Four ultrasound intensities, 47, 57, 67, and 87%, were chosen for this study, which corresponded to P_A values of 58, 70, 83, and 108 μm , respectively. The ultrasonic wave intensities at these four amplitudes were measured calorimetrically by determining the time-dependent change of sample temperature in the ultrasonic reactor as 31, 37, 48, and 62 W/cm^2 according to

$$I = \frac{mC_p}{A} \left[\left(\frac{dT}{dt} \right)_a - \left(\frac{dT}{dt} \right)_b \right] \quad (4)$$

where $(dT/dt)_a$ is the slope of the initial temperature rise and $(dT/dt)_b$ is the slope of heat loss after the ultrasonic reactor was turned off; m is the sample mass, C_p is the heat capacity of the solvent, and A is the end surface area of sonicator probe. Unless specified, all experiments were carried out at an intensity of 48 W/cm², a temperature of 30 °C, a chitosan concentration of 1%, and acetic acid concentration of 1%.

GPC Coupled with Multiangle Laser Light Scattering Detector (MALLS). GPC separations were performed by a Waters 2596 module on three columns (Ultrahydrogel 500, 1000, and 2000; Waters, Milford, MA) with aqueous buffer (0.15 M ammonium acetate/0.2 M acetic acid, 0.02% sodium azide, pH 4.5) as mobile phase at a flow rate of 0.8 mL/min. The column effluent was analyzed by a miniDAWN light scattering detector (Wyatt, Santa Barbara, CA) in series with a refractive index detector (Waters), with the detector outputs analyzed by ASTRA 4 software (Wyatt). The former detector provided measurements of M_w , and the latter detector provided measurements of concentration. The cumulative and differential molecular weight distributions were obtained by ASTRA 5 software. Results from the light scattering detector were analyzed by Zimm plots, and known dn/dc and AUX calibration constants were used for the calculation of molecular weight and radius of gyration. The dn/dc values were adopted from the literature as approximately 0.184, 0.184, 0.185, and 0.187 (L/g) for chitosan samples of 32.5, 30.3, and 20.2% DA and water-soluble chitosan, respectively (19). The GPC samples were prepared as follows: For chitosan samples with $M_w > 100$ kDa the concentration was 0.1% and for samples with $M_w < 100$ kDa the concentration was 0.2%; injection volumes were 100 μ L. The column and RI detector temperature was 30 °C, and the detector cells of MALLS were kept at ambient temperature. Sample solution and mobile phase were filtered through a 0.45 μ m slightly hydrophobic poly(vinylidene difluoride) (PVDF) membrane (Whatman, Clifton, NJ) before use.

Overlap and Entanglement Concentrations. Overlap and entanglement concentrations for chitosan of 32.5% DA were estimated following the method of Cho et al., where the former and latter were defined to be the concentrations at which η equaled $2\eta_s$ and $50\eta_s$, respectively, where η_s is the viscosity of the solvent (20). The viscosity of chitosan solutions was determined by a Cannon–Fenske viscometer at 25 °C with a minimum of three replications performed.

Purification of Sonicated Chitosan for DA Measurement. After 30 min of sonication, the pH of chitosan solutions was adjusted to 10 using 1 M NaOH. The precipitated chitosan was collected by centrifugation, dispersed in deionized water, and centrifuged again. The whole process was repeated three or four times until the pH of the supernatant was 7. The pellets were freeze-dried and stored in a desiccator until further analysis.

DA Measurement. The DA analysis was performed according to the modified first-derivative UV method (21). In short, 100 mg of sample was dissolved by 20 mL of 85% phosphoric acid at 60 °C with stirring for 40 min. The solution was diluted with deionized water (100:1 v/w) and incubated at 60 °C for 2 h before UV analysis. Standard solutions of acetylglucosamine (GlcNAc) and glucosamine (GlcN) were prepared in 0.85% phosphoric acid at concentrations of 0, 10, 20, 30, 40, and 50 μ g/mL. The calibration curve was made by plotting the first derivative of UV values at 203 nm (H203) as a function of the concentrations of GlcNAc and GlcN.

UV Spectra Measurement. UV spectra of solutions of chitosan sonicated at 62 W/cm² for 30 min were collected using a Shimadzu 2010 (Shimadzu, Columbia, MD) double-beam UV–vis spectrophotometer under scan mode in the range from 400 to 190 nm. Sampling interval and slit width were both set at 1.0 nm. Chitosan samples at a concentration of 1% in 1% acetic acid were diluted with deionized water (25:1 v/v) before the UV measurement.

Statistical Analysis and Mathematical Estimation of M_e , k_1 , and k_2 Values. All experiments were repeated three times. ANOVA analysis and significant difference between treatments were determined using Duncan's multiple-range test by SAS program 9.13 (SAS Institute Inc., 2003). Mathcad (PTC, Needham, MA) was used to perform least-

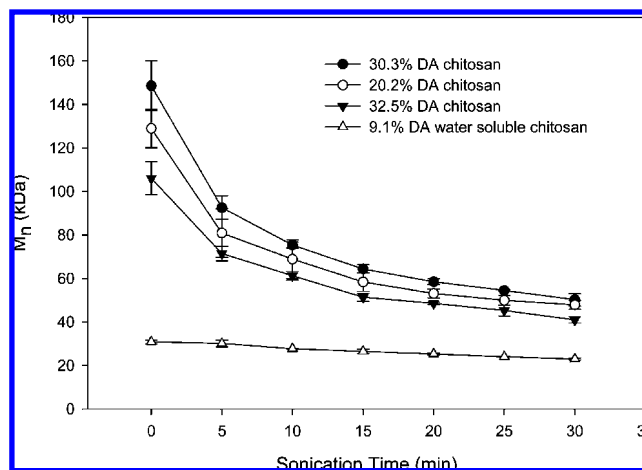


Figure 1. Variation of number-average molecular weight (M_n) with time of sonication for chitosan with different degrees of acetylation and initial molecular weights. Values are represented as mean \pm standard deviation ($n = 3$).

squares analysis to estimate M_e , k_1 (eq 1), and k_3 (eq 3) for random scission and midpoint scission models applied to the M_t versus t data. The best-fit values of M_e , k_1 , and k_3 were found at local minima in the plot of error versus k_1 and M_e and error versus k_3 and M_e , respectively.

RESULTS

Investigation of Models That Describe Sonolysis of Chitosan. As shown in **Figure 1**, the number-average molecular weight, M_n for all chitosan samples decreased with the sonication time at an intensity of 62 W/cm². The determined values of M_n had relatively large standard deviations compared to the values of M_w described later. This is commonly attributed to the interaction between polymer and GPC column stationary phase (22, 23).

To determine which model describes sonolysis of chitosan best, it is necessary to find the final limiting molecular weight M_e of chitosan. To achieve it, a 31 kDa chitosan was sonicated for 3 h, resulting in a final M_n of 17 kDa, which was used as the experimental M_e value to calculate the experimental degradation kinetics. Plots of $\ln[(M_e - M_t)/(M_t - M_i)]$ versus sonication time for the midpoint scission model and $-(M_e/M_t) - \ln[1 - (M_e/M_t)]$ versus sonication time for the random scission model are shown in panels **A** and **B**, respectively, of **Figure 2**. Plotting the values for the midpoint scission model, only the 9.10% DA chitosan gave a straight line (**Figure 2A**), whereas all of the analyzed chitosans gave straight line plots ($R^2 > 0.99$) based on the random scission model (**Figure 2B**).

Because M_e may vary between sonication treatments and the experimentally derived value of 17 kDa might not be universal for all cases, a least-squares analysis was employed to find the best-fit values of M_e for each model and chitosan sample. The results presented in **Table 1** demonstrate that applying numerically derived values of M_e did not affect the correlation coefficients. These results indicated that the ultrasonic degradation of chitosan was not midpoint scission based but rather happened randomly along the chitosan molecule, independent of the method used to estimate the M_e values. Similarly, Baxter et al. found that chitosan was randomly degraded by sonolysis (13); likewise, Tayal and Khan found that ultrasonic degradation of a water-soluble guar galactomannan also followed the random scission model (24). However, another study suggested that the degradation of chitosan by ultrasound was not truly random but was related to the sequence of bond energies: GlcN–GlcN >

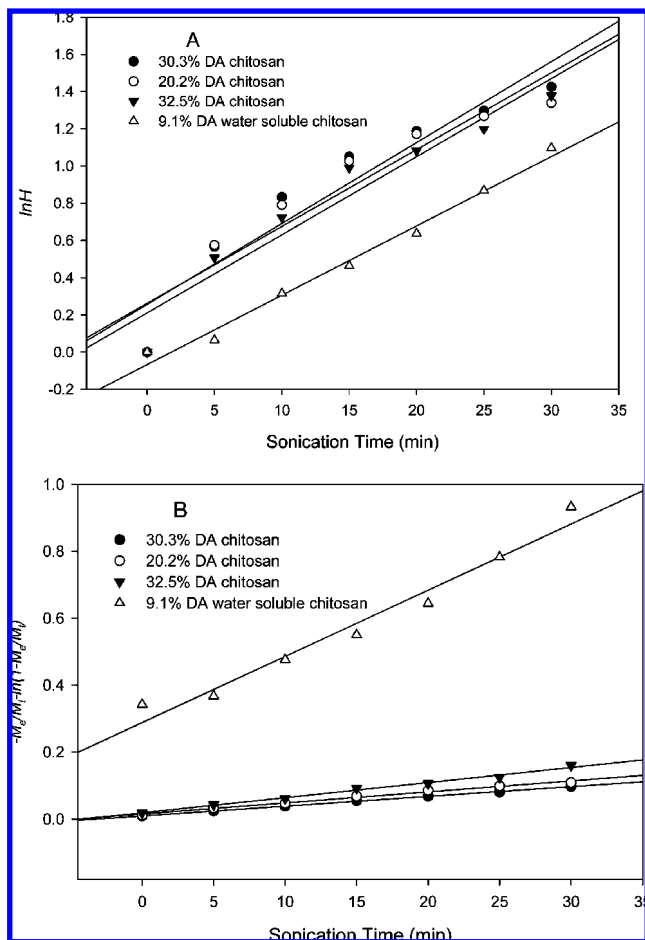


Figure 2. Evaluation of the midscission model (A) and random scission model (B) of chitosan degradation. [$H = (M_t - M_e)/(M_0 - M_e)$] applied to the data plotted in **Figure 1** using experimentally determined values of M_e .

$\text{GlcNAc-GlcN} \approx \text{GlcN-GlcNAc} > \text{GlcNAc-GlcNAc}$ (27). Because the exact distribution of these bonds in a chitosan chain is unknown, the precise site of chain scission cannot be determined. Therefore, our data fit the random scission model better than the midpoint scission model due to the unique copolymer structure of chitosan.

Effect of Molecular Weight on Chitosan Degradation by HIU. The weight-average molecular weights (M_w) before sonication are presented in **Table 2**. The M_w decreased exponentially during sonication for samples with high initial M_w , whereas it decreased linearly for samples with low molecular weight (**Figure 3**). These results indicated that the ultrasound treatment was more efficient for the degradation of high molecular weight chitosan, which was in agreement with previous results (1, 16). Earlier studies has developed the following equation to predict the change of polymer M_w during ultrasonic degradation (17, 29):

$$\frac{1}{(M_w)_t} = \frac{1}{(M_w)_i} + \frac{k_4'}{m}t = \frac{1}{(M_w)_i} + k_4t \quad (5)$$

$(M_w)_t$ is M_w of the polymer after sonication time t , $(M_w)_i$ is the initial M_w of the polymer, m is the molecular weight of the monomer, and k_4' and k_4 are general rate coefficients. A plot of $1/(M_w)_t$ versus the sonication time resulted in a nonlinear relationship (data not shown). However, plots of $1/(M_w)_t^2$ versus sonication time were all linear (inset in **Figure 3**), indicating

Table 1. Degradation Rate Coefficients and Regression Coefficients as a Function of Degree of Acetylation (DA) for Random Chain and Middle Chain Scission Models Using Experimental and Least-Squares Analysis Estimated Final Number-Average Molecular Weight (M_e)

Random Scission (Equation 1)						
DA (%)	M_e (kDa)	$k_1^a \times 10^{11}$ (Da min ⁻¹)	R_1^2	$M_e'^b$ (kDa)	$k_1' \times 10^{11}$ (Da ⁻¹ min ⁻¹)	$R_1'^2$
30.3	17.0	1.34	0.999	36.2	2.27	0.991
20.2	17.0	1.75	0.990	36.8	3.30	0.997
32.5	17.0	2.89	0.991	26.0	3.88	0.986
9.10	17.0	35.2	0.979	1.95	13.2	0.991

Middle Chain Scission (Equation 3)						
DA (%)	M_e (kDa)	$k_3^a \times 10^6$ (Da min ⁻¹)	R_1^2	$M_e'^b$ (kDa)	$k_3' \times 10^4$ (Da ⁻¹ min ⁻¹)	R_2^2
30.3	17.0	2.47	0.901	0.161	2.03 ^c	0.874
20.2	17.0	2.34	0.885	0.161	1.86 ^c	0.856
32.5	17.0	2.35	0.923	0.161	1.77 ^c	0.893
9.10	17.0	1.69	0.991	8.50	1.76	0.992

^a k_1 and k_3 were obtained using the experimentally derived value of M_e at 17.0 kDa. ^b Values of M_e' were estimated for the random scission and midpoint scission models by least-squares analysis. ^c Least-squares analysis resulted in negative M_e and a $M_e = 0.161$ kDa (M_e equals 1 glucosamine monomeric unit) was used to recalculate the k_3' ; R_1^2 and R_2^2 were correlation coefficients of the regression lines plotted in **Figure 11** using the experimentally determined value of M_e and regression lines (data not shown) using least-squares analysis estimated M_e , respectively.

Table 2. Degree of Acetylation (DA) before and after Sonication (30 min, 62 W/cm²) and Initial Weight-Average Molecular Weight (M_w) of Chitosan Samples Used in This Study^a

sample	nominal DA (%)	measured DA (%)	measured DA (%) after sonication	measured M_w (kDa)
40% DA chitosan	39	32.5 ± 0.8	30.0 ± 0.1	221.8 ± 3.3
30% DA chitosan	29	30.3 ± 0.2	28.0 ± 0.7	420.9 ± 1.3
20% DA chitosan	19	20.2 ± 0.1	20.4 ± 0.5	306.8 ± 1.8
water-soluble chitosan		9.10 ± 0.6	9.00 ± 0.1	53.34 ± 0.5

^a Values are represented as mean ± standard deviation ($n = 3$).

that the change of molecular weight could be predicted by the following equation:

$$\frac{1}{(M_w)_t^2} - \frac{1}{(M_w)_i^2} = k_5t \quad (6)$$

Thus, the rate of M_w reduction was actually proportional to the cube of initial molecular weight and could be described by

$$\frac{dM_w}{dt} = -\frac{k_5}{2}M_w^3 \quad (7)$$

It is worth noting that the rate coefficient k_5 is not an absolute rate constant to describe the rate of chitosan chain scission, but rather refers to processing parameters that are associated with the particular reaction conditions, geometry, and ultrasound frequency.

Effect of Degree of Acetylation on Chitosan HIU Degradation. The general rate coefficients k_5 (eq 6) for 32.5, 30.3, and 20.2% DA chitosan were similar, whereas the rate coefficient of 9.10% DA water-soluble chitosan was a factor of 2–3 higher (**Table 3**, experiments 1–4). In contrast, the study of Trzcinski and Staszewska showed that the general rate coefficient decreased with the decrease of degree of acetylation (14). However, a low-intensity ultrasound generator was used in the

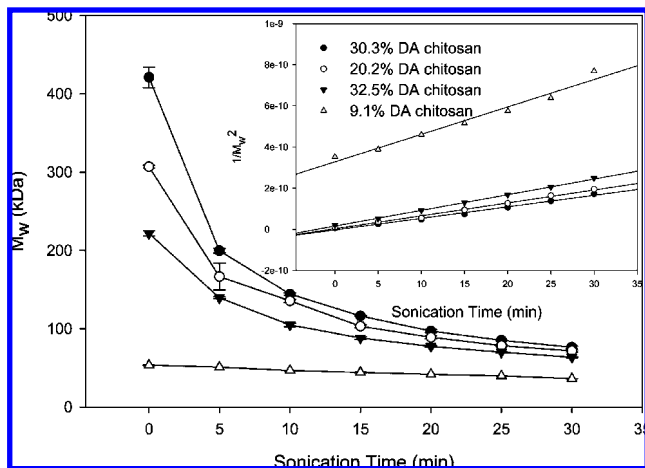


Figure 3. Variation of M_w with sonication time for chitosan with different initial molecular weights and degrees of acetylation. (Inset) $1/(M_w)^2$ versus sonication time. Values are represented as mean \pm standard deviation ($n = 3$).

Table 3. Degradation Rate Coefficients (k_5 , Equation 6) as Affected by Ultrasonic Parameters, Solution Properties, and Degree of Acetylation^a

expt	chitosan			NaCl		$k_5 \times 10^{12}$ ($\text{Da}^{-2} \text{min}^{-1}$)
	DA (%)	intensity (W/cm^2)	concn (% m/v)	temperature ($^\circ\text{C}$)	added acetic acid concn (v/v)	
1	9.10	62	1.00	30	1.00	13.3 ± 0.4
2	20.2	62	1.00	30	1.00	5.35 ± 1.32
3	30.3	62	1.00	30	1.00	5.59 ± 0.24
4	32.5	62	1.00	30	1.00	7.62 ± 0.11
5	20.2	31	1.00	30	1.00	2.03 ± 0.16
6	20.2	37	1.00	30	1.00	2.63 ± 0.03
7	20.2	48	1.00	30	1.00	3.35 ± 0.03
8	20.2	62	1.00	30	1.00	5.35 ± 1.32
9	32.5	48	0.25	30	1.00	11.0 ± 0.4
10	32.5	48	0.50	30	1.00	10.1 ± 0.1
11	32.5	48	1.00	30	1.00	6.75 ± 0.78
12	32.5	48	2.00	30	1.00	3.23 ± 0.12
13	32.5	48	1.00	80	1.00	3.01 ± 0.12
14	32.5	48	1.00	50	1.00	4.66 ± 0.07
15	32.5	48	1.00	30	1.00	6.75 ± 0.78
16	32.5	48	1.00	30	1.00	6.75 ± 0.78
17	32.5	48	1.00	30	0.10	3.71 ± 0.29
18	32.5	48	1.00	30	0.20	3.44 ± 0.31
19	32.5	48	1.00	30	1.00	6.75 ± 0.78
20	32.5	48	1.00	30	2.00	6.26 ± 0.14
21	32.5	48	1.001	30	4.00	6.48 ± 0.20

^a Values are represented as mean value \pm standard error.

cited study, and results might not be directly comparable to the results of **Table 3**, which employed high-intensity ultrasound. In another study the authors observed that the rate coefficients of ultrasound degradation increased with the decrease of chitosan DA and interpreted their results to reflect that highly deacetylated chitosan molecules were more expanded and thus more vulnerable to breakage by shear forces (17). The same study also suggested that the difference in bond energy of β -1,4-glucosidic linkages among different monomer units may be responsible for the experimental observation (17). A recent study, in fact, showed that the hydration energies in the 1,4- β -glucosidic bonds were in the order of $\text{GlcNAc-GlcNAc} > \text{GlcN-GlcNAc} \approx \text{GlcNAc-GlcN} > \text{GlcN-GlcN}$, and the authors proposed that the higher the hydration energy of the bond, the more energy would be needed to break the bond (27). According to the latter, chitosan with lower DA values was more vulnerable to degradation by ultrasound due to lower bond energy (27).

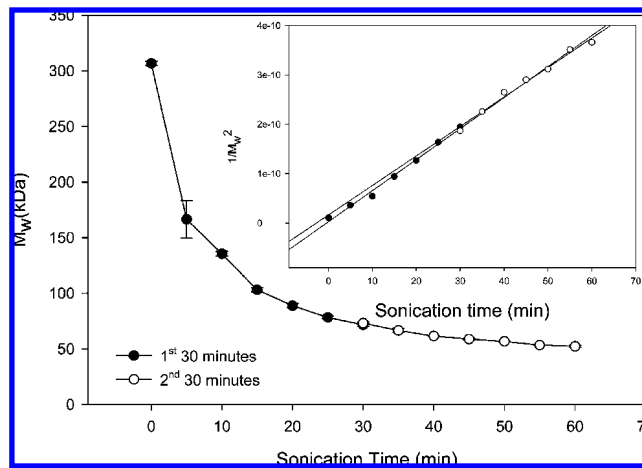


Figure 4. Variation of weight-average molecular weight (M_w) with sonication time for 20.2% degree of acetylation chitosan receiving 30 min of sonication, followed by freeze-drying and sonication for 30 min. (Inset) $1/(M_w)^2$ versus sonication time. Values are represented as mean \pm standard deviation ($n = 3$); rate coefficients k_5 were 5.35×10^{-12} and $5.93 \times 10^{-12} \text{ Da}^{-2} \text{ min}^{-1}$ for the first and second sonications.

At this point we could not conclude that the difference between the rate coefficients (**Table 3**) was caused solely by the difference in DA because the samples also differed in initial M_w . However, the results showed that although the degradation rate was proportional to M_w^3 , the rate coefficient was independent of the initial M_w . When a sonicated sample was collected, freeze-dried, and sonicated for the second time, the decrease of M_w for the second stage continued the trend for the first stage. As shown in **Figure 4**, the degradation of a sample with an initial M_w of 72 kDa maintained the degradation trend of its “parent” molecule with an initial M_w of 307 kDa. The data were horizontally transposed to show the continuous trend in M_w reduction (**Figure 4**), and the $1/M_w^2$ versus time plot (inset in **Figure 4**) reflects the similarity of the rate coefficients (5.35×10^{-12} and $5.93 \times 10^{-12} \text{ Da}^{-2} \text{ min}^{-1}$ for the original and resonicated sample, respectively). Thus, our results indicate that the degradation rate coefficient of chitosan sonication is affected mainly by the DA values. The results showed that only highly deacetylated chitosan (DA 9.10%) was easily degraded, whereas chitosans with DA values in the range of 20.2–32.5% degraded at a slower rate. Similarly, Vijayalakshmi and Madras found that the rate coefficient of sonication degradation was nearly independent of the initial molecular weight of poly(ethylene oxide) (30).

Effect of Free Radical Scavenger on the Chitosan Degradation by Sonolysis. As shown in Figure 1 of the Supporting Information, the degradation processes for 9.10 and 20.2% DA chitosan were identical regardless of the presence of 0.005 mol/L *tert*-butanol in the solutions. *tert*-Butanol is an effective HO^* radical scavenger, and addition of 0.005 mol/L of this compound into the chitosan solution would significantly eliminate the formation of HO^* radicals without affecting the cavitation behavior of ultrasound (10). Czechowska et al. found that the degradation of chitosan by a 360 kHz ultrasound was greatly inhibited with the addition of 0.005 mL/L *tert*-butanol and suggested that ultrasonic degradation at this frequency was the result of both mechanical forces and free radical reactions (10). However, because the addition of *tert*-butanol did not affect the degradation kinetics of chitosans during 20 kHz sonication (Supporting Information Figure 1), we conclude that the ultrasonic degradation under these conditions was only mechanically induced.

Effect of Ultrasound Intensity on the Degradation Process. The influence of ultrasound intensity on the degradation of 20.2% DA chitosan is presented in **Table 3** (experiments 5–8). As expected, the results showed that the rates of ultrasonic degradation increased with an increase of ultrasonic intensity. Similar observations were made by Price and Smith for the degradation of polystyrene (31). A linear relationship was found between the rate coefficient and the ultrasound intensity (Supporting Information Figure 2), and a similar relationship was suggested for chitosan in an earlier study that employed viscosity-average molecular weight (13). The nonzero intercept of this regression line (Supporting Information Figure 2) is consistent with fundamental cavitation physics stating that cavitations are generated only above a certain intensity threshold, referred to as the “cavitation threshold” (18).

Effect of Temperature on the Degradation Process. The influence of solution temperature on the degradation rate of ultrasound was investigated at an intensity of 48 W/cm² at 30, 50, and 80 °C. Samples were sonicated in either ice–water, a room temperature water bath, or ambient air. The degradation rate coefficients decreased with increasing temperature (**Table 3**, experiments 13–15). These results are in agreement with published reports for synthetic polymers and chitosan (1, 14, 31, 32). According to the cavitation physics, cavitation is more active in solvents with lower vapor pressure. Because the vapor pressure of solvents increases with increasing temperature, more solvent molecules may diffuse into the cavities at higher temperatures, thereby dampening the collapse, an effect referred to as “cushioning”. A similar dependence of degradation rate on temperature has been reported for the degradation of polyacrylamide and poly(ethylene oxide) (32).

Effect of Solution Properties on the Degradation Process. The effects of solution properties were investigated by varying the polymer concentration (0.25, 0.5, 1, and 1%), ionic strength (1% chitosan prepared in 1% acetic acid with 0.1 and 0.2 M NaCl), and acetic acid concentration (1% chitosan in 1, 2, an 4% acetic acid).

As presented in **Table 3** (experiments 9–12), the rate coefficients decreased with increasing polymer concentration. This is consistent with published studies of the degradation of synthetic polymers and chitosan (1, 5, 14). With increasing polymer concentration, the viscosity of the solution increases, thereby reducing the extent of the cavitation activity and hence the polymer scission rate (33). The rate coefficients for 0.25 and 0.5% chitosan were similar, suggesting that the increase of the degradation rate due to the decrease of polymer concentration has a limit below which a further reduction in polymer concentration has no effect on the degradation rate. Is this limiting concentration the overlapping (C^*) or entanglement concentration (C_e)? The overlap concentrations of chitosan were reported to be 1.05 g/L (34) and 2.8 g/L (35), depending on the source of chitosan, whereas the entanglement concentrations were reported as 5.0 and 7.4 g/L for chitosan with M_w 8.5×10^5 g/mol depending on the measurement methods (20). In this study, the overlap and entanglement concentrations of the investigated chitosan were determined as 0.27 and 8.87 g/L, respectively. We therefore suggest that the limiting concentration of chitosan is between the overlap concentration and the entanglement concentration, but closer to the latter value. It is likely that as soon as the polymers act as individual molecules, the effect of polymer concentration on ultrasonic degradation becomes insignificant.

As presented in **Table 3** (experiments 16–18), the rate coefficients decreased with the addition of 0.1 and 0.2 M NaCl, respectively. Addition of more than 0.5 M NaCl to the chitosan solution resulted in formation of precipitate, which was at-

tributed to increased hydrophobic interactions, hydrogen bonding, and/or a decrease in electrostatic repulsion (20).

The original ionic strength of the system was based on the contributions of chitosan itself and acetic acid and was calculated to be 0.08 M. With the addition of 0.1 M NaCl, the degradation rate decreased by approximately 50%. Further increases of ionic strength did not cause significant decreases in the rate coefficient. The reduction of the rate coefficient with increasing ionic strength may be explained by the change in the molecular conformation as the chitosan chains may assume a more compact structure with an increase of ionic strength (20). Similar results have been found for the degradation of dextran (5).

The rate coefficients of ultrasonic degradation of 1% chitosan in 1, 2, and 4% acetic acid are presented in **Table 3** (experiments 19–21). The difference between these values is very small, and the effect of acetic acid concentration in this range on the ultrasonic degradation of chitosan appears to be insignificant. As mentioned earlier, the rate of ultrasound degradation was found to be primarily affected by the vapor pressure of a solvent, whereas the effects of solvent viscosity and surface tension are not as pronounced (5). Because the concentration of acetic acid in our study was never more than 4%, we concluded that the effect of acetic acid concentration on the solvent vapor pressure was probably too small to affect the rate of ultrasonic degradation. Furthermore, because the pK_a of chitosan is around 6.3 and the pH for 1% chitosan in 1% acetic acid was 4, the majority of amino groups on chitosan were protonated, and further increases in the acid concentration to 4% did not significantly affect chitosan conformation. Our results were similar to study of Chen et al. (1), whereas Trzcinski et al. reported that the increase of acetic acid concentration caused an increase of general rate parameters (14). The contradictory results of Trzcinski et al. (14) may be caused by different behavior of the system due to the application of a low-power ultrasound emitter with a frequency of 35 kHz and a sonic intensity of 2 W/cm².

Effect of Ultrasound on Radius of Gyration, Polydispersity, Conformation, Molecular Weight Distribution, and Degree of Acetylation of Chitosan. As shown in **Figure 5**, the z -average radius of gyration (**Figure 5A**) and the corresponding polydispersity (**Figure 5B**) all decreased with sonication time. As a result of the molecular weight decrease (**Figure 1**), the decrease of the radius of gyration was expected. The decrease of polydispersity with passage of sonication time has been reported and was attributed to the fact that large molecules are more easily degraded (1).

The differential molecular weight and cumulative molecular weight distribution of 20.2% DA chitosan sonicated at 62 W/cm² are shown in **Figure 6A** and Figure 3 of the Supporting Information, respectively. The cumulative distribution $W(M)$ is defined as the weight fraction of sample having a molar mass of less than M :

$$W(M) = \frac{\sum_{M' < M} C_{M'}}{\sum C_M} \quad (8)$$

where C_M is the mass concentration for the fraction having a molar mass of M' . The differential distribution is defined as

$$X(M) = \frac{dW(M)}{d(\log M)} \quad (9)$$

As seen from both plots, the fractions of low molecular weight chitosan increased, and chitosan with lower polydispersity was obtained with increasing sonication time. The evolution of the mass molecular weight distribution using M_w in this study is consistent with the results using M_n (12).

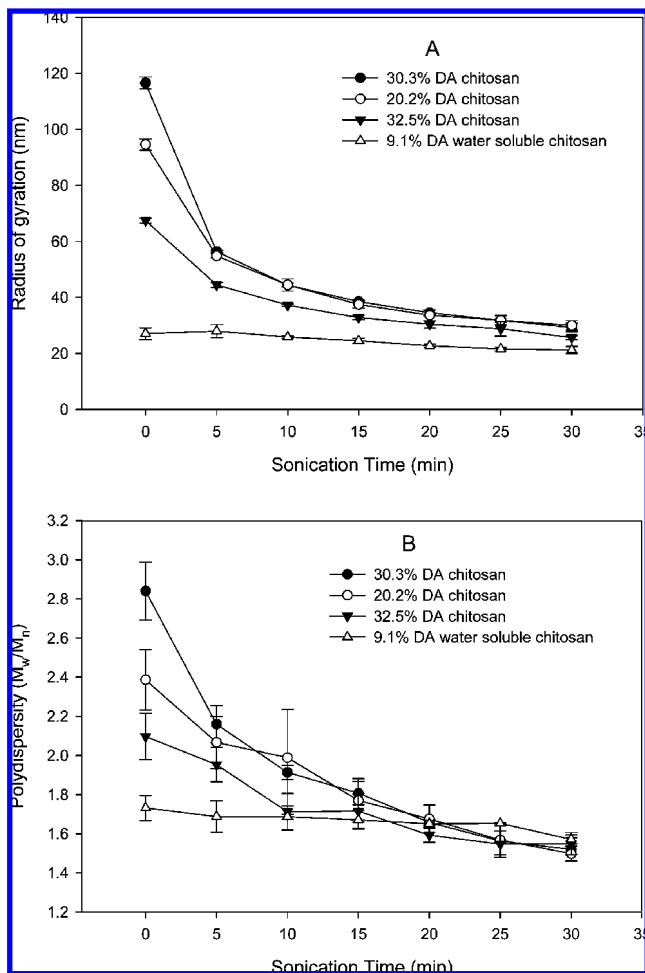


Figure 5. Alteration of radius of gyration and polydispersity of chitosan with sonication time for chitosan with different molecular weights and degrees of acetylation. Values are represented as mean \pm standard deviation ($n = 3$).

Although the molecular weight distribution shifted toward lower molecular weights with increasing sonication time, conformation plots (**Figure 6B**) showed that the majority of chitosan molecules remained in the same conformation after sonication. If a macromolecule of mass M is composed of i elements of mass m , the mean square radius $\langle r_g^2 \rangle$ can be expressed as

$$\langle r_g^2 \rangle = \frac{\sum_i r_i^2 m_i}{\sum_i m_i} = \frac{1}{M} \sum_i r_i^2 m_i \quad (10)$$

where r_i is the distance of element m_i to the mass center of the macromolecule with mass M . The radius can be related to the molar mass M_w by

$$r_g = kM_w^\alpha \quad (11)$$

The plot of $\langle r_g^2 \rangle$ versus the logarithm of the molar mass can be used to determine the slope α , which can provide valuable information about the polymer conformation. Theoretical slopes of 0.33, 0.50, and 1.0 have been described for spheres, random coils, and rigid rods, respectively. The slope α of this plot is related to the Mark–Houwink parameter a by

$$\alpha = (a + 1)/3 \quad (12)$$

Most real random coils have an “ a ” value in the range of 0.55–0.60. The calculated slope of the regression lines for the plots in **Figure 6B** were 0.50 ± 0.02 for chitosan subjected to 0–60

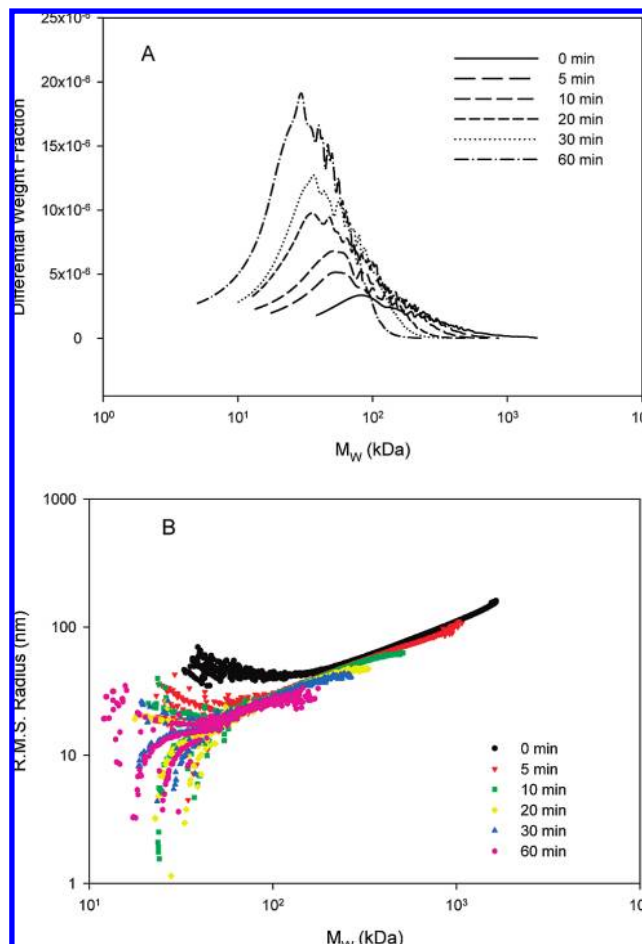


Figure 6. Alteration of differential molecular weight distribution (**A**) and conformation of chitosan (**B**) with sonication time (30.3% DA chitosan).

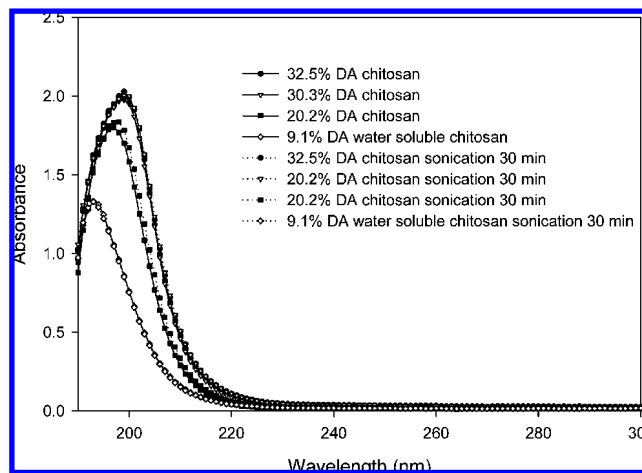


Figure 7. UV spectra of chitosan before and after high-intensity ultrasound treatment for 30 min at 62 W/cm^2 .

min of sonication. The results showed that chitosan remained in a random coil conformation after the sonication regardless of sonication time. This suggests that the degradation is not free radical induced because free radical degradation would result in the formation of macromolecular free radicals, and the recombination of these macromolecular free radicals would likely lead to the formation of side chains and a conformational change.

The UV spectra of chitosan before and after sonication further suggest that degradation was not free radical induced (**Figure 7**). HIU did not alter the UV spectrum of chitosan aqueous solutions

significantly, in contrast to the degradation carried out by a 360 kHz ultrasound, where byproducts containing carbonyl groups were formed as evidenced by a new absorbance peak at 265 nm in the UV spectra (10). This further strengthens the argument that at low frequencies the degradation is mainly due to mechanical forces.

The DA values of chitosan before and after sonication are listed in **Table 2**. ANOVA showed that high-intensity ultrasound treatment had no significant effect on the DA values. Our results are similar to those of Baxter et al. (13), but contrast with those of Liu et al. (16). Liu et al. used a relatively long sonication time compared to our study, which may be the reason for these discrepancies (16).

ACKNOWLEDGMENT

We thank the application scientist, Dr. Myers, at Wyatt Technology Corp. for assistance in obtaining the cumulative and differential molecular weight distributions of chitosan using software ASTRA V.

Supporting Information Available: Degradation processes for 9.10 and 20.2% DA chitosan, relationship between the rate coefficient and the ultrasound intensity, and cumulative molecular weight distribution of 20.2% DA chitosan. This material is available free of charge via the Internet at <http://pubs.acs.org>.

LITERATURE CITED

- Chen, R. H.; Chang, J. R.; Shyur, J. S. Effects of ultrasonic conditions and storage in acidic solutions on changes in molecular weight and polydispersity of treated chitosan. *Carbohydr. Res.* **1997**, *299* (4), 287.
- Ilyina, A. V.; Tikhonov, V. E.; Albulov, A. I.; Varlamov, V. P. Enzymic preparation of acid-free-water-soluble chitosan. *Process Biochem.* **2000**, *35* (6), 563–568.
- Wasikiewicz, J. M.; Yoshii, F.; Nagasawa, N.; Wach, R. A.; Mitomo, H. Degradation of chitosan and sodium alginate by γ radiation, sonochemical and ultraviolet methods. *Radiat. Phys. Chem.* **2005**, *73* (5), 287.
- Hasegawa, M.; Isogai, A.; Onabe, F. Preparation of low-molecular-weight chitosan using phosphoric acid. *Carbohydr. Polym.* **1993**, *20* (4), 279–283.
- Basedow, M. A.; Ebert, H. K. Ultrasonic degradation of polymers in solution. *Adv. Polym. Sci.* **1977**, *22*, 83–148.
- Price, G. Applications of high intensity ultrasound in polymer chemistry. *Chem. Ind.* **1993**, *3*, 75–78.
- Suslick, K. S.; Price, G. J. Applications of ultrasound to materials chemistry. *Annu. Rev. Mater. Sci.* **1999**, *29*, 295–326.
- Mason, T. J.; Lorimer, J. P. *Applied Sonochemistry — The Uses of Power Ultrasound in Chemistry and Processing*; Wiley-VCH Verlag: Weinheim, Germany, 2002.
- Mark, G.; Tauber, A.; Laupert, R.; Schuchmann, H.-P.; Schulz, D.; Mues, A.; von Sonntag, C. OH-radical formation by ultrasound in aqueous solution—part II: terephthalate and Fricke dosimetry and the influence of various conditions on the sonolytic yield. *Ultrason. Sonochem.* **1998**, *5* (2), 41.
- Czechowska-Biskup, R.; Rokita, B.; Lotfy, S.; Ulanski, P.; Rosiak, J. M. Degradation of chitosan and starch by 360-kHz ultrasound. *Carbohydr. Polym.* **2005**, *60* (2), 175–184.
- Schmid, G. Zur Kinetik der Ultraschalldepolymerisation. *Z. Phys. Chem.* **1940**, *186* (3), 113–128.
- Madras, G.; Kumar, S.; Chattopadhyay, S. Continuous distribution kinetics for ultrasonic degradation of polymers. *Polym. Degrad. Stab.* **2000**, *69* (1), 73.
- Baxter, S.; Zivanovic, S.; Weiss, J. Molecular weight and degree of acetylation of high-intensity ultrasonicated chitosan. *Food Hydrocolloids* **2005**, *19* (5), 821.
- Trzcinski, S.; Staszewska, D. U. Kinetics of ultrasonic degradation and polymerisation degree distribution of sonochemically degraded chitosans. *Carbohydr. Polym.* **2004**, *56* (4), 489.
- Li, J.; Du, Y. M.; Yao, P. J.; Wei, Y. A. Prediction and control of depolymerization of chitosan by sonolysis and degradation kinetics. *Acta Polym. Sin.* **2007**, *5*, 401–406.
- Liu, H.; Bao, J.; Du, Y.; Zhou, X.; Kennedy, J. F. Effect of ultrasonic treatment on the biochemophysical properties of chitosan. *Carbohydr. Polym.* **2006**, *64* (4), 553.
- Tsaih, M. L.; Chen, R. H. Effect of degree of deacetylation of chitosan on the kinetics of ultrasonic degradation of chitosan. *J. Appl. Polym. Sci.* **2003**, *90* (13), 3526–3531.
- Kardos, N.; Luche, J.-L. Sonochemistry of carbohydrate compounds. *Carbohydr. Res.* **2001**, *332* (2), 115.
- Sorlier, P.; Rochas, C.; Morfin, I.; Viton, C.; Domard, A. Light scattering studies of the solution properties of chitosans of varying degrees of acetylation. *Biomacromolecules* **2003**, *4*, 1034–1040.
- Cho, J.; Heuzey, M. C.; Begin, A.; Carreau, P. J. Viscoelastic properties of chitosan solutions: Effect of concentration and ionic strength. *J. Food Eng.* **2006**, *74* (4), 500.
- Wu, T.; Zivanovic, S. Determination of the degree of acetylation (DA) of chitin and chitosan by an improved first derivative UV method. *Carbohydr. Polym.* **2008**, *73* (2), 248–253.
- Barth, H. G.; Boyes, B. E.; Jackson, C. Size exclusion chromatography. *Anal. Chem.* **1996**, *68*, 445–466.
- Barth, H. G.; Boyes, B. E.; Jackson, C. Size exclusion chromatography and related separation techniques. *Anal. Chem.* **1998**, *70*, 251–278.
- Tayal, A.; Khan, S. A. Degradation of a water-soluble polymer: molecular weight changes and chain scission characteristics. *Macromolecules* **2000**, *33*, 9488–9493.
- Kurita, K.; Sannan, T.; Iwakura, Y. Studies on chitin, 4. Evidence for formation of block and random copolymers of *N*-acetyl-D-glucosamine and D-glucosamine by hetero- and homogeneous hydrolyses. *Makromol. Chem.* **1977**, *178* (12), 3197–3202.
- Berkowski, K. L.; Potisek, S. L.; Hickenboth, C. R.; Moore, J. S. Ultrasound-induced site-specific cleavage of azo-functionalized poly(ethylene glycol). *Macromolecules* **2005**, *38*, 8975–8978.
- Liu, H.; Du, Y. M.; Kennedy, J. F. Hydration energy of the 1,4-bonds of chitosan and their breakdown by ultrasonic treatment. *Carbohydr. Polym.* **2007**, *68* (3), 598–600.
- Cravotto, G.; Omiccioli, G.; Stevanato, L. An improved sonochemical reactor. *Ultrason. Sonochem.* **2005**, *12* (3), 213–217.
- Portenlanger, G.; Heusinger, H. The influence of frequency on the mechanical and radical effects for the ultrasonic degradation of dextrans. *Ultrason. Sonochem.* **1997**, *4*, 127–130.
- Vijayalakshmi, S. P.; Madras, G. Effect of initial molecular weight and solvents on the ultrasonic degradation of poly(ethylene oxide). *Polym. Degrad. Stab.* **2005**, *90* (1), 116–122.
- Price, G. J.; Smith, P. F. Ultrasonic degradation of polymer solutions: 2. The effect of temperature, ultrasound intensity and dissolved gases on polystyrene in toluene. *Polymer* **1993**, *34* (19), 4111.
- Vijayalakshmi, S. P.; Madras, G. Effect of temperature on the ultrasonic degradation of polyacrylamide and poly(ethylene oxide). *Polym. Degrad. Stab.* **2004**, *84* (2), 341.
- Kuijpers, M. W. A.; Prickaerts, R. M. H.; Kemmere, M. F.; Keurentjes, J. T. F. Influence of the CO₂ antisolvent effect on ultrasound-induced polymer scission kinetics. *Macromolecules* **2005**, *38*, 1493–1499.
- Desbrieres, J. Viscosity of semiflexible chitosan solutions: influence of concentration, temperature, and role of intermolecular interactions. *Biomacromolecules* **2002**, *3*, 342–349.
- Hwang, J. K.; Shin, H. H. Rheological properties of chitosan solutions. *Korea–Aust. Rheol. J.* **2000**, *12* (3/4), 175–179.

Received for review October 25, 2007. Revised manuscript received March 5, 2008. Accepted April 16, 2008. This research was supported by USDA NRI Grant 2005-35503-15428 and Hatch funds from the Tennessee Experiment Station TEN264.